JACS
JOURNAL OF THE AMERICAN CHEMICAL SOCIETY
Article
pubs.acs.org/JACS

Fast Negative Photochromism of 1,1′-Binaphthyl-Bridged Phenoxyl−Imidazolyl Radical Complex

Tetsuo Yamaguchi, Yoichi Kobayashi, and Jiro Abe*

Department of Chemistry, School of Science and Engineering, Aoyama Gakuin University, 5-10-1 Fuchinobe, Chuo-ku, Sagamihara, Kanagawa 252-5258, Japan

Supporting Information

ABSTRACT: Negative photochromism, in which a thermally stable colored form isomerizes to the transient colorless form by light irradiation and the back reaction occurs thermally, is advantageous in its applications for photoswitching materials because visible light can cause the photochromic color change of the materials. Moreover, the photochromic color change can be induced even on the inside of the materials due to the absence of the reabsorption of the visible excitation light by the photogenerated colorless species. While several negative photochromic compounds have been reported, the time scales of the back reaction are still slower than minutes, and no available fast responsive negative photochromic compounds have been reported. Here, we developed a negative photochromic 1,1′-binaphthyl-bridged phenoxyl−imidazolyl radical complex (BN-PIC) which enables fast photoswitching by visible light. The stable colored BN-PIC shows instantaneous decoloration by visible light irradiation, and the photogenerated colorless form thermally reverts to the initial colored form with a half-life of 1.9 s at room temperature. BN-PIC can also cause the drastic change in the chiroptical properties by the photochromic reaction, and the rate of the thermal back reaction is affected by the chirality of the solvent. Since the negative photochromic reaction can occur on the inside of the materials, the fast negative photochromism is expected to have an impact in the fields of photoresponsive materials of solid states and molecular aggregates.

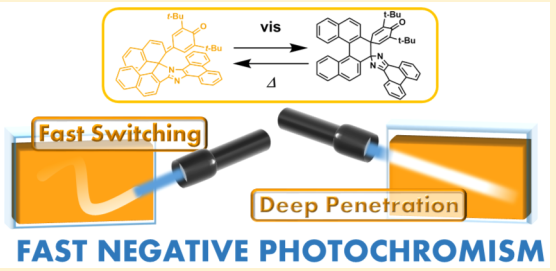

INTRODUCTION

Photochromic compounds have been applied to various fields of science and technology because of their high functionalities and versatilities.[1−4] In conventional T-type photochromic compounds, the colorless or less colored form is a stable isomer and it isomerizes to the thermally unstable colored form upon UV light irradiation. Although conventional T-type photochromic compounds have been demonstrated as a promising material for various applications, one of the serious issues is reabsorption of the excitation UV light by the photogenerated colored form. That is, the photochromic reaction can occur only near the surface of the materials. This issue becomes prominent in bulk materials such as crystals, films, and liquid crystals. If the photogenerated species does not absorb the excitation light, the light goes deep inside the materials and induces the photochromic reactions on the inside of the materials. One of the best candidates for overcoming this issue is the use of negative photochromic compounds. Negative photochromism is a photochromic reaction in which the thermally stable colored form isomerizes to the metastable colorless form upon visible light irradiation, and the generated colorless form thermally returns to the initial colored form.[5−8] There are several reports on negative photochromic compounds such as spiropyran derivatives,[9−11] dimethyldihydropyrenes,[12,13] Stenhouse salts,[14,15] and 1,1′-binaphthyl-bridged imidazole dimers.[16] The time scales of the thermal back reaction of these negative photochromic reactions range from minutes to hours to days, and no fast response negative photochromic compounds have been demonstrated until today.

The potential of the acceleration of the thermal back reaction in T-type photochromic compounds has been demonstrated by bridged imidazole dimers,[17−19] pentaarylbiimidazole (PABI),[20] phenoxyl−imidazolyl radical complex (PIC),[21] and so on.[22−24] By accelerating the thermal back reaction from seconds to sub-microseconds, the potential applications of these photochromic compounds have expanded from photochromic lenses to dynamic holography,[25,26] security systems, and fast fluorescence switching for super-resolution microscopy.[27,28] As already demonstrated by the fast photochromic molecules, the acceleration of the thermal back reaction of negative photochromism is expected to initiate novel potentials of negative photochromic materials.

In this study, we report the fast photoswitchable negative photochromism of 1,1′-binaphthyl-bridged phenoxyl−imidazolyl radical complex (BN-PIC, Scheme 1). The strategy for the molecular design of BN-PIC was inspired by the molecular frameworks of PIC and 1,1′-binaphthyl-bridged imidazole dimer. Upon light irradiation, the colored and colorless forms of BN-PICs give the short-lived biradical species that forms either colored or colorless forms by the intramolecular radical

Received: October 19, 2015
Published: December 29, 2015

DOI: 10.1021/jacs.5b10924
J. Am. Chem. Soc. 2016, 138, 906−913

Scheme 1. Photochromic Reaction of (a) BN-PIC1 and (b) BN-PIC2

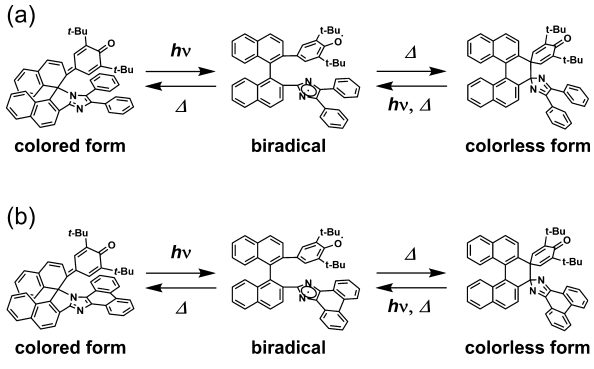

coupling reaction. **BN-PIC1** shows a slow thermal back reaction from the photogenerated colorless form to the thermally stable colored form via the thermally accessible biradical species, while **BN-PIC2**, in which the diphenylimidazole moiety is replaced with the phenanthroimidazole moiety, greatly accelerates the thermal back reaction to a time scale of seconds. In addition to the negative photochromic properties of BN-PICs, the unique chiroptical properties are also demonstrated.

RESULTS AND DISCUSSION

The molecular structures of the stable colored forms of **BN-PIC1** and **BN-PIC2** were revealed by X-ray crystallographic analysis, as shown in Figure 1a,b. Their structures are similar to those of the previously reported 1,1′-binaphthyl-bridged imidazole dimers in terms of the C−N bond formation between the nitrogen atom of the imidazole ring and the carbon atom of the 1-position of the naphthalene moiety.[16,25]

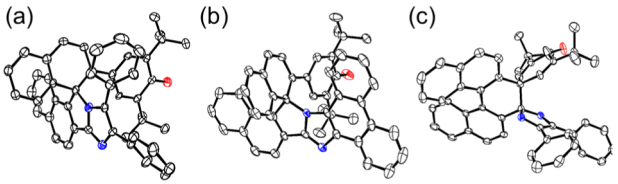

Figure 1. ORTEP representations of the (a) colored form of **BN-PIC1**, (b) colored form of **BN-PIC2**, and (c) colorless form of **BN-PIC1** with thermal ellipsoids (50% probability), where nitrogen and oxygen atoms are highlighted in blue and red, respectively. The hydrogen atoms, the solvent molecules, and the disorders of *tert*-butyl and carbonyl groups of the colorless form of **BN-PIC1** are omitted for clarity.

The UV−vis absorption spectra of the colored forms of **BN-PIC1** and **BN-PIC2** are similar to each other, as shown in Figure 2. The calculated absorption spectra obtained by the density functional theory (DFT) are consistent with the experimental spectra. The colored forms of **BN-PIC1** and **BN-PIC2** have a broad absorption band from the UV region to 500 nm. The DFT calculations suggest that these absorption bands are attributed to the $\pi-\pi^*$ transition around the cyclohexadienone moiety (Figures S60 and S66).

The photochromic response was not observed in the crystalline states of the colored forms of **BN-PIC1** and **BN-PIC2**. On the other hand, they show reversible color changes in solution upon visible light irradiation ascribed to negative photochromism; that is, BN-PICs show the decoloration reaction upon visible light irradiation, and the photogenerated colorless species thermally revert to the initial colored forms. Though the crystals of the colorless form of **BN-PIC2** could not be obtained due to the fast thermal back reaction leading to the formation of the stable colored form, visible light irradiation at −40 °C on the saturated solution (dichloromethane/acetonitrile = 1/6) of the colored form of **BN-PIC1** gave crystals of the colorless form. Moreover, the single crystal of the colorless form of **BN-PIC1** colorizes to yellow upon continued heating overnight at 60 °C, indicating the occurrence of the thermal back reaction in the crystal. The molecular structure of the colorless form of **BN-PIC1** was revealed by X-ray crystallographic analysis, as shown in Figure 1c. The similarity in the molecular framework and the negative photochromic behavior of **BN-PIC2** indicates that the colorless form of **BN-PIC2** is considered to have a molecular structure similar to that of **BN-PIC1**.

The absorption spectra of **BN-PIC1** and **BN-PIC2** in benzene just after visible light irradiation are shown in the center of Figure 2a,b, respectively. The spectra were measured by using a multichannel photodiode array ultraviolet−visible detector to reduce the effect of the thermal back reaction on the spectral measurements. The absorbance in the visible region of the colored form of **BN-PIC1** completely disappeared upon visible light irradiation with a 100 W Xe lamp at 25 °C, whereas that of **BN-PIC2** remained slightly at the same irradiation conditions due to the faster recovery of the colored form. The calculated absorption spectra are in fair agreement with the experimental spectra. As shown in Figure 2, the time profiles of the recovery of the absorbance in the visible region of the colorless solutions of **BN-PIC1** and **BN-PIC2** follow the first-order kinetics (Figures S26 and S28). The half-lives of the colorless forms are estimated to be 10.9 min at 40 °C and 1.9 s at 25 °C for **BN-PIC1** and **BN-PIC2**, respectively. The decay kinetics of the colorless forms were not affected by the presence of molecular oxygen (Figure S30). It should be emphasized that the thermal back reaction of **BN-PIC2** is the fastest among the so far reported negative photochromic systems that take more than minutes (Movie S1).

Figure 3 shows the temperature dependence of the thermal back reaction measured over the temperature ranges from 25 to 50 °C for **BN-PIC1** and from 5 to 40 °C for **BN-PIC2**. As described below, the thermal back reaction proceeds via the thermally accessible biradical species. Therefore, the activation parameters ($\Delta H^{\ddagger}$, $\Delta S^{\ddagger}$, and $\Delta G^{\ddagger}$) for the thermal back reaction derived from the Eyring equation (Figures S27 and S29) are only apparent values. The $\Delta H^{\ddagger}$, $\Delta S^{\ddagger}$, and $\Delta G^{\ddagger}$ values at 25 °C for the thermal back reaction of **BN-PIC1** are 99.8 kJ mol^{-1}, 16.4 J K^{-1} mol^{-1}, and 94.9 kJ mol^{-1}, respectively. The corresponding values for **BN-PIC2** are 77.2 kJ mol^{-1}, 6.16 J K^{-1} mol^{-1}, and 75.4 kJ mol^{-1}, respectively.

Previous studies have revealed that the photoisomerization from the colored to colorless forms of 1,1′-binaphthyl-bridged imidazole dimers occurs via a short-lived biradical species.[16] To investigate whether the biradical species is involved in the negative photochromism of BN-PICs, transient absorption spectra were measured by using a 355 nm nanosecond laser pulse as an excitation light source. As shown in Figure 4, the transient absorption spectra of the stable colored forms of BN-PICs show a large bleach signal from 400 to 500 nm due to the depletion of the ground state population and a broad absorption band longer than 500 nm in both compounds. The absorption minimum of each bleach signal corresponds to

DOI: 10.1021/jacs.5b10924
J. Am. Chem. Soc. 2016, 138, 906−913

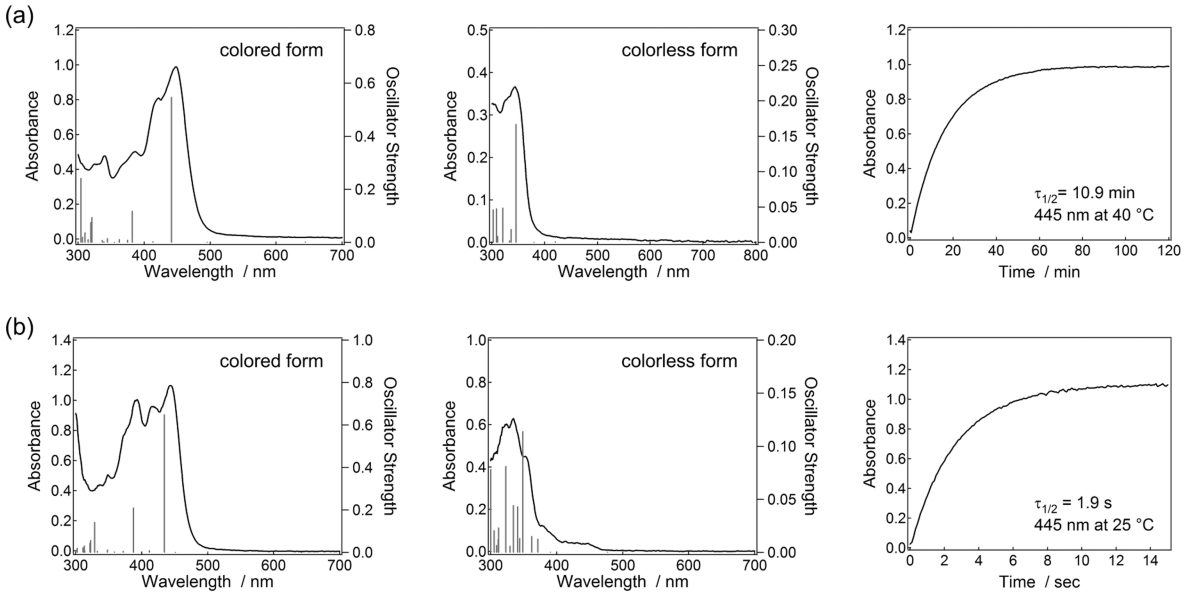

Figure 2. (a) UV−visible absorption spectra of the colored form (left), the colorless form (center), and the time profile of the absorbance changes at 445 nm of the solution of the colorless form obtained by visible light irradiation (right) of **BN-PIC1** in degassed benzene (3.2×10^{-5} M), and (b) those of **BN-PIC2** in degassed benzene (3.0×10^{-5} M). The measurement of the time profiles was carried out at 40 °C for **BN-PIC1** and at 25 °C for **BN-PIC2**. The calculated absorption spectra (DFT MPW1PW91/6-31+G(d,p)//M052X/6-31G(d,p)) are shown by the vertical lines.

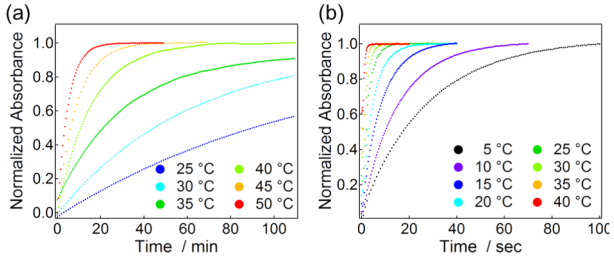

Figure 3. Temperature dependence of the time profiles of the absorbance changes at 445 nm of the solution of the colorless form obtained by visible light irradiation of (a) **BN-PIC1** in degassed benzene (3.0×10^{-5} M) and (b) **BN-PIC2** in degassed benzene (2.2×10^{-5} M).

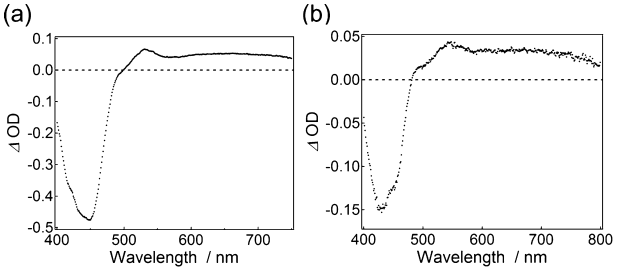

Figure 4. Transient vis−NIR absorption spectra of the colored forms of (a) **BN-PIC1** in degassed benzene solution (2.4×10^{-5} M) and (b) **BN-PIC2** in degassed benzene solution (2.3×10^{-5} M) at 25 °C. The spectra were recorded at 10 ns after excitation with a nanosecond laser pulse (excitation wavelength, 355 nm; pulse duration, 5 ns; power, 7 mJ/pulse).

the peak top of the absorption spectra of the colored forms. Although the transient absorption spectra at the shorter wavelength are overlapped with the negative bleach signal, the broad positive transient absorption signal at the longer wavelength looks similar to that of the biradical species reported previously. By considering the similarity of the photochromic property of BN-PICs and those of the bridged imidazole dimers,[16,29,30] we assigned the positive transient signal to the absorption signal of the biradical species.

To reveal the whole spectral shapes of the biradical species, we performed the measurements of the transient absorption spectra of the colorless forms of both compounds at low temperature, where the thermal back reaction of the colorless forms populated by visible light irradiation can be suppressed. Under the low-temperature condition, it is not necessary to take into account the bleach signal due to the depletion of the ground state population of the colorless form because the colorless form has no absorption bands longer than 400 nm, as shown in Figure 2. The transient absorption spectra of the colorless forms were measured at −50 °C for **BN-PIC1** and at −80 °C for **BN-PIC2**. Figure 5a,b shows the transient absorption spectra that is attributable to the biradical species of **BN-PIC1** and **BN-PIC2**, respectively. The spectral shapes longer than 500 nm are the same as those obtained for the colored form. Moreover, we confirmed that the decay kinetics of the radical species do not show a significant difference regardless of the composition between the colored and the colorless forms. These experimental results strongly support that the colored and colorless forms of BN-PICs give the same biradical species upon light irradiation. The half-lives of the biradical species generated from **BN-PIC1** and **BN-PIC2** were estimated to be 380 and 240 ns, respectively (Figure 5). The effect of molecular oxygen on the half-life of the biradical species was negligibly small (Figures S35 and S36).

As described above, the colorless forms can be obtained upon visible light irradiation to the solution of the colored form of BN-PICs. On the other hand, UV light irradiation to the colorless forms of BN-PICs give only a trace of the colored form. Thus, the major reaction path for the deactivation of the biradical species is the formation of the colorless form, suggesting the difference in the activation energy barriers for the formation of each isomer. Thus, the negative photochromic behavior of BN-PICs includes three isomers and can be

DOI: 10.1021/jacs.5b10924
J. Am. Chem. Soc. 2016, 138, 906−913

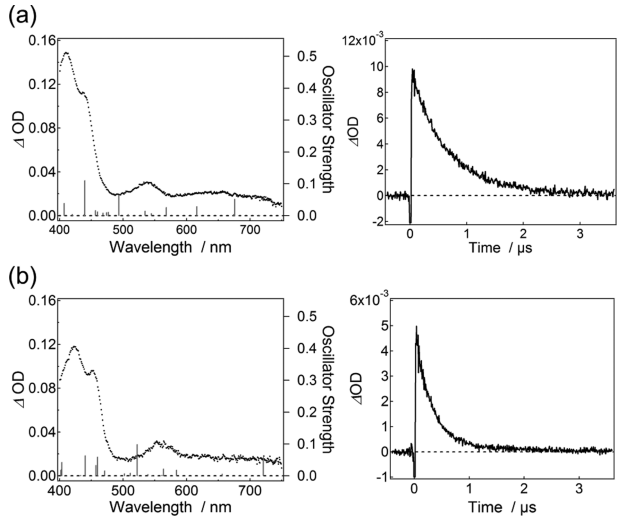

Figure 5. (a) Vis−NIR transient absorption spectrum recorded at 1 μs after the excitation with a nanosecond 355 nm laser pulse (4 mJ/pulse) at −50 °C for the colorless degassed toluene solution (1.3×10^{-4} M) of **BN-PIC1** (left). Transient absorption profile of **BN-PIC1** in degassed benzene (2.4×10^{-5} M) at 25 °C excited with nanosecond 355 nm laser pulses (7.5 mJ/pulse) and probed at 650 nm (right). (b) Vis−NIR transient absorption spectrum recorded at 1 μs after the excitation with a nanosecond 355 nm laser pulse (4 mJ/pulse) at −80 °C for the colorless degassed toluene solution (9.1×10^{-5} M) of **BN-PIC2** (left). Transient absorption profile of **BN-PIC2** in degassed benzene (2.3×10^{-5} M) at 25 °C excited with nanosecond 355 nm laser pulses (7.5 mJ/pulse) and probed at 650 nm (right). The calculated absorption spectra (DFT UMPW1PW91/6-31+G(d,p)//UM052X/6-31G(d,p)) of the singlet spin state of the biradical species are shown by the perpendicular lines.

explained by Scheme 1. The thermally stable colored forms isomerize to the colorless forms via the short-lived biradical species by visible light irradiation. The colorless forms isomerize slightly to the colored forms via the radical species by UV light irradiation. The photogenerated colorless forms thermally return to the initial colored forms with time scales of minutes and seconds for **BN-PIC1** and **BN-PIC2**, respectively.

The photochemical conversion efficiencies from the colored forms to the colorless forms of **BN-PIC1** and **BN-PIC2** were estimated by nanosecond laser flash photolysis by using 1,2-bis(2-methylbenzo[*b*]thiophen-3-yl)perfluorocyclopentene[31] (DAE) as a standard. The colorless open-ring isomer of DAE can undergo cyclization in a conrotatory fashion to the colored closed-ring isomer upon UV light irradiation. The thermal back reaction is symmetry-forbidden, giving excellent thermal stability to the closed-ring isomer. The cycloreversion reaction from the closed-ring isomer to the open-ring isomer occurs only by irradiation with a visible light. The quantum yield of the ring-opening reaction of DAE at 436 nm was estimated to be 0.45 by using potassium trisoxalatoferrate(III) trihydrate as a chemical actinometer. Solutions of the colored forms of BN-PICs in benzene and the closed-ring isomer of DAE in hexane with matched absorbances at the excitation wavelength of 436 nm were irradiated at various laser energies. The absorbance changes for the colored form of BN-PIC, ΔOD(BN-PIC), were plotted against those before and after a laser pulse irradiation at 436 nm for the closed-ring isomer of DAE, ΔOD(DAE). The conversion efficiency was estimated from the slope of the fit of the data to the following equation:[32,33]

$$\Delta\mathrm{OD(BN\text{-}PIC)} = \frac{\phi_{\mathrm{BN\text{-}PIC}} \times \varepsilon_{\mathrm{BN\text{-}PIC}}}{\phi_{\mathrm{DAE}} \times \varepsilon_{\mathrm{DAE}}} \Delta\mathrm{OD(DAE)} \quad (1)$$

where, φ_{DAE} (0.45) is the quantum yield of the cycloreversion reaction of DAE excited at 436 nm, $\varphi_{\mathrm{BN\text{-}PIC}}$ is the conversion efficiency from the colored form to the colorless form of BN-PIC, $\varepsilon_{\mathrm{DAE}}$ (3.50×10^3 M^{-1} cm^{-1}) and $\varepsilon_{\mathrm{BN\text{-}PIC}}$ (2.73×10^4 M^{-1} cm^{-1} for **BN-PIC1**, 3.39×10^4 M^{-1} cm^{-1} for **BN-PIC2**) are the absorptivity coefficients of DAE and the colored forms of BN-PICs at 436 nm, respectively. As shown in Figures S46 and S47, $\varphi_{\mathrm{BN\text{-}PIC1}}$ and $\varphi_{\mathrm{BN\text{-}PIC2}}$ were obtained from the slopes of the fits of the data to eq 1 and were determined to be 0.09 and 0.08,

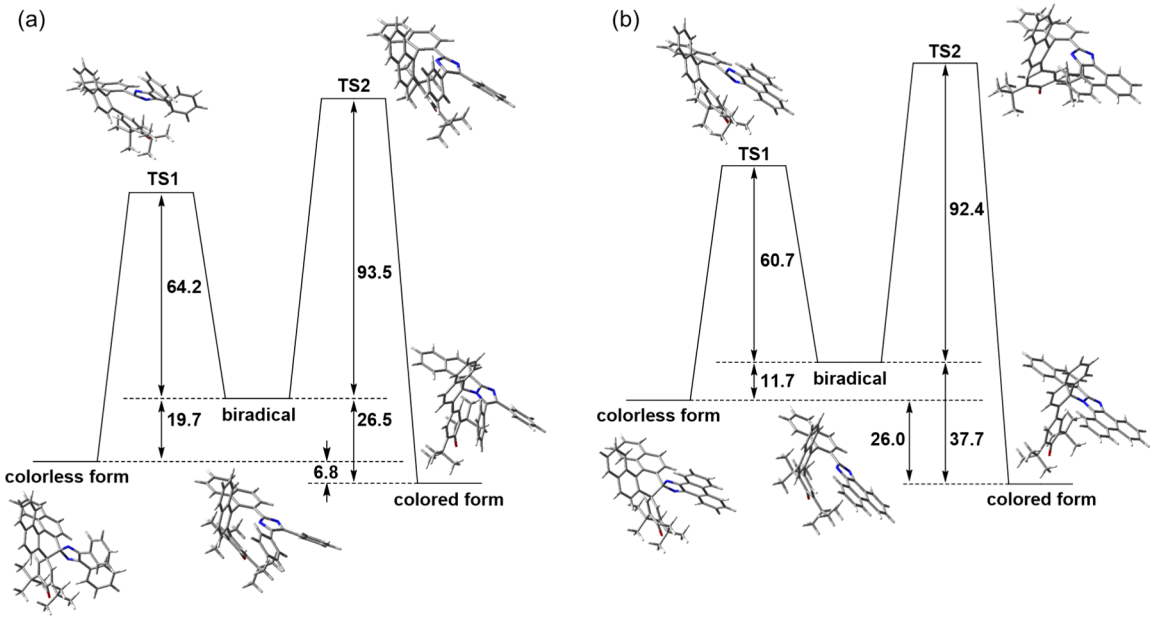

Figure 6. Energy diagrams for the thermal back reactions and the optimized molecular structures of (a) **BN-PIC1** and (b) **BN-PIC2** calculated by the DFT M05-2X/6-31G(d,p). The Gibbs free energies at 298.15 K are given in the unit of kJ mol^{-1}.

DOI: 10.1021/jacs.5b10924
J. Am. Chem. Soc. 2016, 138, 906−913

respectively. The full experimental data are shown in the Supporting Information. These values were nearly 3 times higher than that of the previously reported negative photochromic 1,1′-binaphthyl-bridged imidazole dimer.[16]

We carried out the DFT calculations to understand the photochemical and thermochemical isomerization behavior of BN-PICs. The molecular geometries of the colored form, the colorless form, and the biradical species were fully optimized at the M05-2X/6-31G(d,p) level of the theory. The time-dependent DFT calculations were performed at the MPW1PW91/6-31+G(d,p) level of the theory for the optimized geometries obtained by the M05-2X/6-31G(d,p) method. Moreover, the transition states for the radical coupling reaction were investigated to understand the difference in the activation energy barriers for the formation of each isomer. The stationary nature of the structures was confirmed by harmonic vibrational frequency calculations; that is, equilibrium species possess all real frequencies, whereas transition states possess only one imaginary frequency. The M05-2X function is known to give improved performance for energies of reactions involving radicals, for barrier heights of radical reactions.[34] The Gibbs free energy barriers, $\Delta G^{\ddagger}$, of the radical coupling reaction of [2.2]paracyclophane-bridged imidazole dimers were in fair agreement with the experimental values.[18] The calculated energy diagrams for **BN-PIC1** and **BN-PIC2** are shown in Figure 6a,b, respectively. The experimental observations can be well accounted for by the DFT calculations.

First, the colored forms are more stable than the colorless forms. Second, the activation energy barriers for the formation of the colorless forms are smaller than those for the formation of the colored forms. That is why the major reaction path for the deactivation of the biradical species is the formation of the colorless form, and the colorless forms isomerize slightly to the colored forms via the radical species by UV light irradiation. The colorless form gradually isomerizes to the colored form because the colored form is produced from the biradical species by the thermodynamic controlled reaction, whereas the formation of the colorless form is the kinetic controlled reaction. Third, both of the activation energy barriers for the formation of the biradical species and the colored form of **BN-PIC2** are smaller than those of **BN-PIC1**, leading to the faster thermal back reaction of **BN-PIC2** compared with that of **BN-PIC1**. Thus, the photochemical and thermochemical isomerization behavior of BN-PICs can be well described by the energy diagrams obtained by the DFT calculations.

As described in the Introduction, negative photochromic compounds are promising not only because of their unique photochromic property but also because of the potential to induce the photochromism on the inside of the material. Therefore, the combination of a negative photochromic property with other properties would open up the possibility for developments of novel highly functional materials. BN-PICs have an axial chirality that originated from the 1,1′-binaphthyl structure. Here, as a demonstration, we investigated the effect of the chiral environment on the thermal back reaction of the optically resolved **BN-PIC1**. We chose **BN-PIC1** as an example because **BN-PIC1** and **BN-PIC2** have similar molecular structures and **BN-PIC1** is easy to analyze because of its slow thermal back reaction from the photogenerated colorless form to the thermally stable colored form. Both enantiomers of **BN-PIC1** were optically resolved by using chiral HPLC, and the optical purities were up to 97 and 99% ee for *R*- and *S*-enantiomers, respectively (Figure S52). Circular dichroism

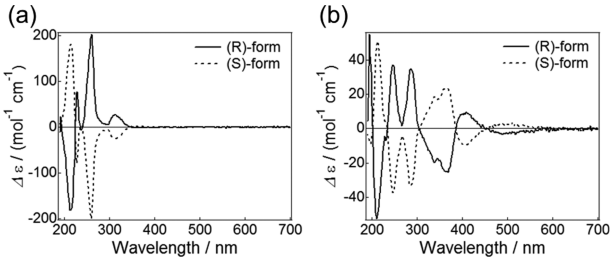

Figure 7. CD spectra of the (a) colored forms and (b) colorless forms of **BN-PIC1** in aerated acetonitrile at 25 °C. The CD spectra of the colorless forms were measured after a sufficient amount of visible light irradiation.

(CD) spectra of the colored forms of **BN-PIC1** are shown in Figure 7a. The colored forms of **BN-PIC1** in acetonitrile show CD signals from UV to the visible region. This spectrum indicates that the chiroptical property that originated from the 1,1′-binaphthyl unit expands over the cyclohexadienone moiety. Upon visible light irradiation, the CD signal in the visible region disappeared and the strong CD signal due to the colorless form was observed at the UV region (Figure 7b). Since it is known that the 1,1′-binaphthyl moiety exhibits a positive Cotton effect around 300 nm,[35] we assigned the enantiomer of the colorless form, which gives a positive Cotton effect around 300 nm to the (*R*)-form (Figures 7b). The colored enantiomer that returned from the (*R*)-colorless form is also regarded as the (*R*)-colored form in this study. The CD spectrum of the photogenerated colorless form gradually reverts to the initial CD spectrum that is assigned to the colored form in the dark (Figure S54). Furthermore, the (*S*)-colored form was not racemized by continuous irradiation of 365 nm UV light for 1 min (100 mW) as was revealed by the chiral HPLC analyses (Figure S53). These results show that the negative photochromism of **BN-PIC1** also induces the drastic change of the chiroptical property, and the enantiomers are not photoracemized by continuous light irradiation.

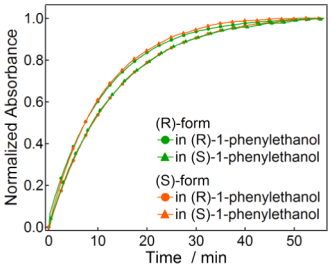

Figure 8. Time profiles of the absorbance during the thermal back reactions from the colorless to the colored forms of the enantiomers of **BN-PIC1** in aerated (*R*)-1-phenylethanol and (*S*)-1-phenylethanol at 25 °C.

Moreover, the thermal back reaction from the colorless to colored forms is found to be affected by the solvent chirality. Figure 8 shows the time evolution of the absorbance of **BN-PIC1** during the thermal back reaction from the colorless to the colored forms in different chirality of 1-phenylethanol (see also Figure S55). The kinetics of the (*R*)-form in the (*R*)-solvent is obviously different from that of the (*R*)-form in the (*S*)-solvent. The kinetics of the (*S*)-form in the (*S*)-solvent follows the kinetics of the (*R*)-form in the (*R*)-solvent. Alternatively, the kinetics of the (*R*)-form in the (*S*)-solvent follows the kinetics

DOI: 10.1021/jacs.5b10924
J. Am. Chem. Soc. 2016, 138, 906−913

Scheme 2. Synthetic Scheme of BN-PIC1 and BN-PIC2

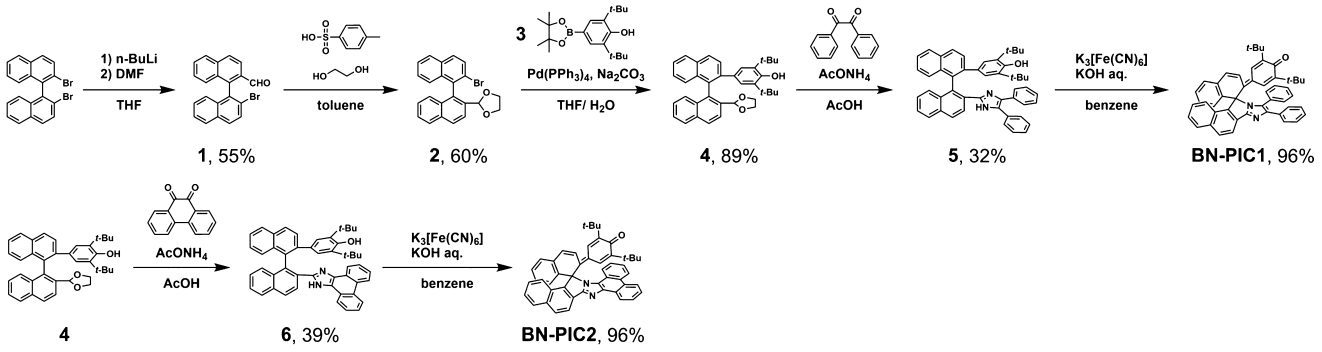

of the (*S*)-form in the (*R*)-solvent. Although the difference is small, these results clearly show that the thermal back reaction of **BN-PIC1** is affected by the chiral environment of the solvent. While there are many examples where the chiral environment affects the reaction products of the enantiomer excess,[36−39] this is an unusual behavior of the thermal back reaction of negative photochromism affected by the chiral environment.[40,41] The activation parameters of the (*S*)- and (*R*)-forms in each enantiomer of 1-phenylethanol were analyzed by the Eyring equation (Figures S56 and S57). The $\Delta G^{\ddagger}$ value of the thermal back reaction for the (*S*)-form in (*S*)-1-phenylethanol at 25 °C (89.2 kJ mol^{-1}) was slightly smaller than that for the (*S*)-form in (*R*)-1-phenylethanol (89.5 kJ mol^{-1}). This is also the case for the kinetics of the (*R*)-form in (*R*)-1-phenylethanol (89.1 kJ mol^{-1}) and the (*R*)-form in (*S*)-1-phenylethanol (89.5 kJ mol^{-1}).

CONCLUSION

We have developed the novel negative photochromic molecules, **BN-PIC1** and **BN-PIC2**. The negative photochromic behavior of BN-PICs includes three isomers, that is, the colored form, the colorless form, and the biradical species. The colored and colorless forms of BN-PICs give the same biradical species upon light irradiation. The major reaction path for the deactivation of the biradical species is the formation of the colorless form. The thermally stable colored forms isomerize to the colorless forms via the biradical species by visible light irradiation, whereas the colorless forms isomerize slightly to the colored forms via the radical species by UV light irradiation. The thermal back reaction from the photogenerated colorless form to the colored form takes 10.9 min at 40 °C and 1.9 s at 25 °C for **BN-PIC1** and **BN-PIC2**, respectively.

Furthermore, CD spectroscopy revealed that the negative photochromism of BN-PICs induces the large change in the chiroptical property. Since negative photochromism can induce the photochromic reaction deep inside the material, which cannot be achieved in conventional photochromism, the fast negative photochromic systems with large changes in their chiroptical properties associated with the photochromic reaction are useful for photomechanical materials, real-time holographic materials, and photoresponsive chiral dopants for liquid crystals.

EXPERIMENTAL SECTION

Synthesis. All reactions were monitored by thin-layer chromatography carried out on 0.2 mm E. Merck silica gel plates (60F-254). Column chromatography was performed on silica gel (Wakogel C-300). All reagents and solvents were obtained from commercial suppliers (Sigma-Aldrich, Wako Chemicals, TCI, Kanto Chemical Company, Inc., and Acros Organics), and the reagents were used without further purification. All reaction solvents were distilled on the appropriate drying reagents prior to use. ^{1}H NMR spectra and ^{13}C NMR spectra were recorded on a Bruker AVANCE III 400NanoBay at 400 and 100 MHz, respectively. Chemical shifts (δ) are recorded in parts per million (ppm) relative to tetramethylsilane, and the coupling constants (J) are reported in Hertz (Hz). DMSO-d_6 and $CDCl_3$ were used as deuterated solvents. Mass spectra (ESI-TOF-MS) were recorded on a Bruker micrOTOF II-AGA1. The synthetic sequences of **BN-PIC1** and **BN-PIC2** are outlined in Scheme 2.

*2′-Bromo-[1,1′-binaphthalene]-2-carbaldehyde (**1**).* 2,2′-Dibromo-1,1′-binaphthyl (995 mg, 2.4 mmol) was dissolved in 13.4 mL of dry THF and cooled to −78 °C. *n*-Butyllithium (1.6 M, 1.6 mL) was added dropwise to the reaction mixture and stirred for 1 h. After addition of the dry DMF, the mixture was stirred for 1 h and another 2.5 h at room temperature. HCl (1 N) was added and stirred for 1 h. The reaction mixture was washed with water and extracted with ethyl acetate. The organic extracts were evaporated and purified using column chromatography on silica gel (CH_2Cl_2/hexane = 1/1) to yield **1** as a pale yellow solid (483 mg, 55%): ^{1}H NMR (400 MHz, $CDCl_3$) δ 9.63 (s, 1H), 8.18 (d, J = 8.7 Hz, 1H), 8.08 (d, J = 8.6 Hz, 2H), 8.00 (d, J = 8.3 Hz, 1H), 7.95 (d, J = 8.2 Hz, 1H), 7.93 (d, J = 9.0 Hz, 1H), 7.84 (d, J = 8.8 Hz, 1H), 7.63 (t, J = 7.4 Hz, 1H), 7.52 (t, J = 7.4 Hz, 1H), 7.37 (t, J = 7.6 Hz, 1H), 7.30 (t, J = 7.7 Hz, 1H), 7.25 (d, J = 7.4 Hz, 1H), 7.04 (d, J = 8.5 Hz, 1H); m/z (HR-ESI-TOF-MS) calcd for $C_{21}H_{13}BrO$ [M + Na]$^{+}$ 383.0042, found 383.0035.

*2-(2′-Bromo-[1,1′-binaphthalen]-2-yl)-1,3-dioxolane (**2**).* 2′-Bromo-[1,1′-binaphthalene]-2-carbaldehyde (**1**) (203 mg, 0.56 mmol), *p*-toluenesulfonic acid (5 mg, 0.028 mmol), ethylene glycol (0.080 mL, 1.4 mmol), and toluene (5.6 mL) were added and refluxed for 2 days. After being cooled to room temperature, the reaction mixture was washed with water and extracted with ethyl acetate and concentrated. The residue was purified using column chromatography on silica gel (CH_2Cl_2/hexane = 1/1) to yield **2** as a pale yellow solid (136 mg, 60%): ^{1}H NMR (400 MHz, $CDCl_3$) δ 8.06 (d, J = 8.6 Hz, 1H), 7.95 (d, J = 8.0 Hz, 1H), 7.92 (d, J = 8.2 Hz, 1H), 7.88−7.79 (m, 3H), 7.50 (t, J = 7.6 Hz, 2H), 7.32−7.27 (m, 2H), 7.13 (d, J = 8.4 Hz, 1H), 7.05 (d, J = 8.2 Hz, 1H), 5.36 (s, 1H), 4.18−4.04 (m, 2H), 3.90−3.70 (m, 2H); m/z (HR-ESI-TOF-MS) calcd for $C_{23}H_{17}O_2BrNa$ [M + Na]$^{+}$ 427.0304, found 427.0285.

*4-(2′-(1,3-Dioxolan-2-yl)-[1,1′-binaphthalen]-2-yl)-2,6-di-tert-butylphenol (**4**).* 2-(2′-Bromo-[1,1′-binaphthalen]-2-yl)-1,3-dioxolane (**2**) (52 mg, 0.13 mmol), 2,6-di-*tert*-butyl-4-(4,4,5,5-tetramethyl-1,3,2-dioxaborolan-2-yl)phenol (**3**)[21] (59 mg, 0.18 mol), sodium carbonate (63 mg, 0.59 mmol), tetrakis(triphenylphosphine)palladium (0) (13 mg, 0.011 mmol), THF (0.65 mL), and water (0.26 mL) were added to a sealed tube. The reaction mixture was degassed by three freeze−pump−thaw cycles and refluxed for overnight. After Celite filtration, the filtrate was washed with water and extracted with ethyl acetate. The organic layer was dried in vacuo, and the residue was purified using column chromatography on silica gel (CH_2Cl_2/hexane = 1/1) to yield **4** as a white solid (58 mg, 89%): ^{1}H NMR (400 MHz, $CDCl_3$) δ 8.03 (d, J = 8.5 Hz, 1H), 7.94 (d, J = 8.4 Hz, 1H), 7.82 (t, J = 8.6 Hz, 2H), 7.69 (d, J = 8.5 Hz, 1H), 7.61 (d, J = 8.7 Hz, 1H), 7.45

DOI: 10.1021/jacs.5b10924
J. Am. Chem. Soc. 2016, 138, 906−913

(t, J = 7.3 Hz, 1H), 7.39 (t, J = 7.3 Hz, 1H), 7.25−7.20 (m, 5H), 6.79 (s, 2H), 4.90 (s, 1H), 4.05−3.92 (m, 2H), 3.73−3.64 (m, 2H), 1.09 (s, 18H); m/z (HR-ESI-TOF-MS) calcd for $C_{37}H_{38}O_3Na$ $[M + Na]^+$ 553.2713, found 553.2811.

*2,6-Di-tert-butyl-4-(2′-(4,5-diphenyl-1H-imidazol-2-yl)-[1,1′-binaphthalen]-2-yl)phenol (**5**).* 4-(2′-(1,3-Dioxolan-2-yl)-[1,1′-binaphthalen]-2-yl)-2,6-di-*tert*-butylphenol (**4**) (58 mg, 0.11 mmol), benzil (29 mg, 0.14 mmol), ammonium acetate (207 mg, 2.66 mmol), and acetic acid (1.5 mL) were added to a sealed tube and refluxed for 1 day. The resulting mixture was cooled to room temperature and neutralized with aqueous NH_3. The residue was filtered and dried in vacuo. The crude product was purified using column chromatography on silica gel (CH_2Cl_2/hexane = 3/1) to yield **5** as a pale yellow solid (24 mg, 32%): ^{1}H NMR (400 MHz, DMSO-d_6) δ 11.48 (s, 1H), 8.16 (d, J = 8.5 Hz, 1H), 8.11 (d, J = 8.9 Hz, 1H), 8.06 (d, J = 8.5 Hz, 1H), 8.01 (d, J = 8.3 Hz, 1H), 7.99 (d, J = 6.8 Hz, 1H), 7.64 (d, J = 8.3 Hz, 1H), 7.49 (t, J = 7.1 Hz, 1H), 7.43 (t, J = 7.3 Hz, 1H), 7.40−7.33 (m, 3H), 7.32−7.26 (m, 4H), 7.23 (t, J = 7.5 Hz, 1H), 7.10−7.06 (m, 4H), 7.05−7.00 (m, 2H), 6.60 (s, 2H), 6.51 (s, 1H), 0.88 (s, 18H); m/z (HR-ESI-TOF-MS) calcd for $C_{49}H_{45}N_2O$ $[M + H]^+$ 677.3526, found 677.3523.

BN-PIC1. A water solution (4.0 mL) containing potassium ferricyanide (416 mg, 1.3 mmol) and KOH (135 mg, 2.4 mmol) was added to a benzene solution (4.0 mL) of 2,6-di-*tert*-butyl-4-(2′-(4,5-diphenyl-1*H*-imidazol-2-yl)-[1,1′-binaphthalen]-2-yl)phenol (**5**) (24 mg, 0.035 mmol). After being stirred for 1.5 h at room temperature, the resultant mixture was then extracted with benzene and the organic extract was washed with water. After removal of the solvents, the crude product was purified by reverse phase HPLC using CH_3CN as the eluent to yield **BN-PIC1** as an orange solid (23 mg, 96%): ^{1}H NMR (400 MHz, $CDCl_3$) δ 8.25 (d, J = 8.3 Hz, 1H), 8.02 (d, J = 8.3 Hz, 1H), 7.88 (d, J = 8.2 Hz, 1H), 7.54 (t, J = 8.5 Hz, 3H), 7.39 (t, J = 7.2 Hz, 1H), 7.30 (t, J = 7.2 Hz, 1H), 7.27−7.00 (m, 11H), 6.84 (d, J = 10.2 Hz, 1H), 6.79 (d, J = 8.0 Hz, 1H), 6.50 (d, J = 4.87 Hz, 3H), 1.20 (s, 9H), 0.93 (s, 9H); ^{13}C NMR (100 MHz, $CDCl_3$) δ 185.97, 151.31, 150.83, 148.91, 147.73, 142.76, 140.67, 137.33, 134.56, 134.00, 133.12, 130.81, 130.66, 130.63, 130.28, 130.07, 129.69, 129.48, 128.65, 128.15, 128.12, 128.07, 128.05, 127.78, 127.27, 126.93, 126.58, 126.54, 126.44, 126.33, 126.21, 123.84, 122.85, 118.28, 68.44, 35.77, 35.48, 29.61, 29.48; m/z (HR-ESI-TOF-MS) calcd for $C_{49}H_{43}N_2O$ $[M + H]^+$ 675.3370, found 675.3363.

*4-(2′-(1H-Phenanthro[9,10-d]imidazol-2-yl)-[1,1′-binaphthalen]-2-yl)-2,6-di-tert-butylphenol (**6**).* 4-(2′-(1,3-Dioxolan-2-yl)-[1,1′-binaphthalen]-2-yl)-2,6-di-*tert*-butylphenol (**4**) (51 mg, 0.096 mmol), 9,10-phenanthrenequinone (24 mg, 0.12 mmol), ammonium acetate (270 mg, 3.5 mmol), and acetic acid (1.3 mL) were added to a sealed tube and refluxed for 1 day. The resulting mixture was cooled to room temperature and neutralized with aqueous NH_3. The residue was filtrated and dried in vacuo. The crude product was purified using column chromatography on silica gel (CH_2Cl_2/hexane = 2/1) to yield **6** as a pale yellow solid (25 mg, 39%): ^{1}H NMR (400 MHz, DMSO-d_6) δ 12.80 (s, 1H), 8.76 (d, J = 7.8 Hz, 1H), 8.70 (d, J = 8.5 Hz, 1H), 8.40 (d, J = 8.2 Hz, 1H), 8.20−8.04 (m, 5H), 7.68−7.42 (m, 10H), 7.26 (t, J = 7.9 Hz, 1H), 7.17 (d, J = 8.7 Hz, 1H), 6.47 (s, 3H), 0.76 (s, 18H); m/z (HR-ESI-TOF-MS) calcd for $C_{49}H_{43}N_2O$ $[M + H]^+$ 675.3370, found 675.3380.

BN-PIC2. A water solution (1.7 mL) containing potassium ferricyanide (179 mg, 0.54 mmol) and KOH (76 mg, 1.4 mmol) was added to a benzene solution (1.7 mL) of 4-(2′-(1*H*-phenanthro-[9,10-d]imidazol-2-yl)-[1,1′-binaphthalen]-2-yl)-2,6-di-*tert*-butylphenol (**6**) (10 mg, 0.015 mmol). After being stirred for 1 h at room temperature, the resultant mixture was then extracted with benzene and the organic extract was washed with water. After removal of the solvents, **BN-PIC2** was given without further purification as an orange solid (10 mg, 96%): ^{1}H NMR (400 MHz, $CDCl_3$) δ 8.82 (t, J = 8.6 Hz, 2H), 8.75 (d, J = 7.8 Hz, 1H), 8.38 (d, J = 8.4 Hz, 1H), 8.29 (d, J = 7.9 Hz, 1H), 8.27 (d, J = 9.9 Hz, 1H), 8.14 (dd, J_1= 2.6, J_2= 7.5 Hz, 1H), 7.87−7.76 (m, 4H), 7.73−7.65 (m, 3H), 7.60−7.51 (m, 3H), 7.43 (t, J = 7.6 Hz, 1H), 7.21 (t, J = 7.7 Hz, 1H), 6.91 (t, J = 7.9 Hz, 1H), 6.62 (s, 1H), 6.34 (d, J = 8.3 Hz, 1H), 1.11 (s, 9H), 0.67 (s, 9H); ^{13}C NMR (100 MHz, $CDCl_3$) δ 186.00, 156.25, 152.82, 149.05, 148.50, 143.15, 138.89, 135.67, 134.73, 133.99, 131.47, 131.38, 130.97, 130.22, 129.71, 128.76, 128.63, 128.41, 128.34, 128.18, 128.13, 128.02, 127.88, 127.25, 126.75, 126.41, 126.30, 126.07, 125.67, 125.56, 125.16, 124.97, 124.57, 123.71, 123.24, 123.09, 122.74, 122.49, 122.25, 118.49, 35.64, 35.60, 29.55, 29.39; m/z (HR-ESI-TOF-MS) calcd for $C_{49}H_{41}N_2O$ $[M + H]^+$ 673.3213, found 673.3171.

Laser Flash Photolysis Measurements. The laser flash photolysis experiments were carried out with a time-resolved spectrophotometer (TSP-2000, Unisoku Co., Ltd.). The samples were excited by a Q-switched Nd:YAG laser (Continuum Minilite II; 355 nm, pulse duration: 5 ns). The probe beam from a halogen lamp (OSRAM HLX64623) was focused into the sample to be arranged in an orientation perpendicular to the exciting laser beam. The probe beam was monitored with a photomultiplier tube (Hamamatsu R2949) through a spectrometer (Unisoku MD2000). To obtain the transient absorption spectra of the biradical species, we measured the transient absorption spectra of the colorless forms at low temperature (−50 and −80 °C for **BN-PIC1** and **BN-PIC2**, respectively). Before the transient absorption measurements, a halogen lamp was irradiated for several minutes to convert the initial colored forms to the colorless forms at low temperature. A Xe flash lamp (Hamamatsu L2437, pulse duration: ∼2 μs) and ICCD-spectrometer combination (Andor iStar DH320T-18U-03 and Shamrock 163) were used for a probe light and detector, respectively. The gate duration of the ICCD was set to 20 ns, and a spectrum was obtained by the average of 150 scans (average of the 50 scans, then the halogen light was irradiated to the sample, and these procedures were repeated three times to exclude the effect of the thermal back reaction from the colorless to colored forms). We confirmed that the thermal back reaction from the colorless to colored forms is negligible during the experiments under those temperatures.

■ ASSOCIATED CONTENT

Supporting Information

The Supporting Information is available free of charge on the ACS Publications website at DOI: 10.1021/jacs.5b10924.

^{1}H and ^{13}C NMR spectra, MS spectra, X-ray crystallographic analysis data, HPLC chromatograms, spectroscopic measurements, measurements for conversion efficiency, DFT calculations (PDF)

Movie S1 (AVI)

X-ray data for $C_{51}H_{45}N_3O$ (CIF)

X-ray data for $C_{49}H_{42}N_2O$ (CIF)

X-ray data for $C_{53}H_{48}N_2O_3$ (CIF)

■ AUTHOR INFORMATION

Corresponding Author

*jiro_abe@chem.aoyama.ac.jp

Notes

The authors declare no competing financial interest.

■ ACKNOWLEDGMENTS

This work was supported partly by the Core Research for Evolutionary Science and Technology (CREST) program of the Japan Science and Technology Agency (JST) and a Grant-in-Aid for Scientific Research on Innovative Areas "Photosynergetics" (No. 26107010) from MEXT, Japan. Financial assistance for this research was also provided by the MEXT-Supported Program for the Strategic Research Foundation at Private Universities, 2013−2017. T.Y. appreciates the Research Fellowships of JSPS for Young Scientists.

■ REFERENCES

(1) Irie, M.; Yokoyama, Y.; Seki, T. *New Frontiers in Photochromism*; Springer: Japan, 2013.

DOI: 10.1021/jacs.5b10924
J. Am. Chem. Soc. 2016, 138, 906−913

(2) Feringa, B. L.; Browne, W. R. *Molecular Switches*; Wiley-VCH Verlag: Weinheim, Germany, 2011.
(3) Düerr, H.; Bouas-Laurent, H. *Photochromism: Molecules and Systems*; Elsevier: Amsterdam, 2003.
(4) Crano, J. C.; Guglielmetti, R. J. *Organic Photochromic and Thermochromic Compounds*; Plenum Press: New York, 1999.
(5) Ubukata, T.; Takahashi, K.; Yokoyama, Y. *J. Phys. Org. Chem.* **2007**, *20*, 981−984.
(6) Ciardelli, F.; Fabbri, D.; Pieroni, O.; Fissi, A. *J. Am. Chem. Soc.* **1989**, *111*, 3470−3472.
(7) Fissi, A.; Pieroni, O.; Ruggeri, G.; Ciardelli, F. *Macromolecules* **1995**, *28*, 302−309.
(8) Roldan, D.; Cobo, S.; Lafolet, F.; Vilà, N.; Bochot, C.; Bucher, C.; Saint-Aman, E.; Boggio-Pasqua, M.; Garavelli, M.; Royal, G. *Chem. - Eur. J.* **2015**, *21*, 455−467.
(9) Tanaka, M.; Ikeda, T.; Xu, Q.; Ando, H.; Shibutani, Y.; Nakamura, M.; Sakamoto, H.; Yajima, S.; Kimura, K. *J. Org. Chem.* **2002**, *67*, 2223−2227.
(10) Minami, M.; Taguchi, N. *Chem. Lett.* **1996**, *25*, 429−430.
(11) Tomasulo, M.; Yildiz, I.; Raymo, F. M. *Inorg. Chim. Acta* **2007**, *360*, 938−944.
(12) Mitchell, R. H.; Ward, T. R.; Chen, Y.; Wang, Y.; Weerawarna, S. A.; Dibble, P. W.; Marsella, M. J.; Almutairi, A.; Wang, Z. Q. *J. Am. Chem. Soc.* **2003**, *125*, 2974−2988.
(13) Bohne, C.; Mitchell, R. H. *J. Photochem. Photobiol., C* **2011**, *12*, 126−137.
(14) Honda, K.; Komizu, H.; Kawasaki, M. *J. Chem. Soc., Chem. Commun.* **1982**, 253−254.
(15) Helmy, S.; Leibfarth, F. A.; Oh, S.; Poelma, J. E.; Hawker, C. J.; Read de Alaniz, J. *J. Am. Chem. Soc.* **2014**, *136*, 8169−8172.
(16) Hatano, S.; Horino, T.; Tokita, A.; Oshima, T.; Abe, J. *J. Am. Chem. Soc.* **2013**, *135*, 3164−3172.
(17) Kishimoto, Y.; Abe, J. *J. Am. Chem. Soc.* **2009**, *131*, 4227−4229.
(18) Harada, Y.; Hatano, S.; Kimoto, A.; Abe, J. *J. Phys. Chem. Lett.* **2010**, *1*, 1112−1115.
(19) Iwasaki, T.; Kato, T.; Kobayashi, Y.; Abe, J. *Chem. Commun.* **2014**, *50*, 7481−7484.
(20) Yamashita, H.; Abe, J. *Chem. Commun.* **2014**, *50*, 8468−8471.
(21) Yamashita, H.; Ikezawa, T.; Kobayashi, Y.; Abe, J. *J. Am. Chem. Soc.* **2015**, *137*, 4952−4955.
(22) Arai, K.; Kobayashi, Y.; Abe, J. *Chem. Commun.* **2015**, *51*, 3057−3060.
(23) Tomasulo, M.; Sortino, S.; Raymo, F. M. *Org. Lett.* **2005**, *7*, 1109−1112.
(24) Garcia-Amorós, J.; Bučinskas, A.; Reig, M.; Nonell, S.; Velasco, D. *J. Mater. Chem. C* **2014**, *2*, 474−480.
(25) Ishii, N.; Kato, T.; Abe, J. *Sci. Rep.* **2012**, *2*, 819.
(26) Ishii, N.; Abe, J. *Appl. Phys. Lett.* **2013**, *102*, 163301.
(27) Deniz, E.; Tomasulo, M.; Cusido, J.; Sortino, S.; Raymo, F. M. *Langmuir* **2011**, *27*, 11773−11783.
(28) Deniz, E.; Tomasulo, M.; Cusido, J.; Yildiz, I.; Petriella, M.; Bossi, M. L.; Sortino, S.; Raymo, F. M. *J. Phys. Chem. C* **2012**, *116*, 6058−6068.
(29) Yamaguchi, T.; Hatano, S.; Abe, J. *J. Phys. Chem. A* **2014**, *118*, 134−143.
(30) Yamaguchi, T.; Hilbers, M. F.; Reinders, P. P.; Kobayashi, Y.; Brouwer, A. M.; Abe, J. *Chem. Commun.* **2015**, *51*, 1375−1378.
(31) Hanazawa, M.; Sumiya, R.; Horikawa, Y.; Irie, M. *J. Chem. Soc., Chem. Commun.* **1992**, 206−207.
(32) Wintgens, V.; Johnston, L. J.; Scaiano, J. C. *J. Am. Chem. Soc.* **1988**, *110*, 511−517.
(33) Sheepwash, M. A. L.; Ward, T. R.; Wang, Y.; Bandyopadhyay, S.; Mitchell, R. H.; Bohne, C. *Photochem. Photobiol. Sci.* **2003**, *2*, 104−112.
(34) Zhao, Y.; Truhlar, D. G. *J. Phys. Chem. A* **2008**, *112*, 1095−1099.
(35) Mislow, K.; Bunnenberg, E.; Records, R.; Wellman, K.; Djerassi, C. *J. Am. Chem. Soc.* **1963**, *85*, 1342−1349.
(36) Inoue, Y. *Chem. Rev.* **1992**, *92*, 741−770.
(37) North, M.; Villuendas, P. *Org. Lett.* **2010**, *12*, 2378−2381.
(38) Ding, J.; Desikan, V.; Han, X.; Xiao, T. L.; Ding, R.; Jenks, W. S.; Armstrong, D. W. *Org. Lett.* **2005**, *7*, 335−337.
(39) Baudequin, C.; Brégeon, D.; Levillain, J.; Guillen, F.; Plaquevent, J. C.; Gaumont, A. C. *Tetrahedron: Asymmetry* **2005**, *16*, 3921−3945.
(40) Yamamoto, S.; Matsuda, K.; Irie, M. *Org. Lett.* **2003**, *5*, 1769−1772.
(41) Fukagawa, M.; Kawamura, I.; Ubukata, T.; Yokoyama, Y. *Chem. - Eur. J.* **2013**, *19*, 9434−9437.

DOI: 10.1021/jacs.5b10924
J. Am. Chem. Soc. 2016, 138, 906−913